

# Nonlinear self-interaction induced black hole bomb

Cheng-Yong Zhang<sup>1,\*</sup>, Qian Chen<sup>2,†</sup>, Yuxuan Liu<sup>3,‡</sup>, Yu Tian<sup>2,4,§</sup>, Bin Wang<sup>5,6,¶</sup> and Hongbao Zhang<sup>7,8,\*\*\*</sup>

<sup>1</sup>College of Physics and Optoelectronic Engineering, Jinan University, Guangzhou 510632, China

<sup>2</sup>School of Physical Sciences, University of Chinese Academy of Sciences, Beijing 100049, China

<sup>3</sup>School of Physics and Electronics, Central South University, Changsha 418003, China

<sup>4</sup>Institute of Theoretical Physics, Chinese Academy of Sciences, Beijing 100190, China

<sup>5</sup>Center for Gravitation and Cosmology, College of Physical Science

and Technology, Yangzhou University, Yangzhou 225009, China

<sup>6</sup>School of Aeronautics and Astronautics, Shanghai Jiao Tong University, Shanghai 200240, China

<sup>7</sup>Department of Physics, Beijing Normal University, Beijing 100875, China

<sup>8</sup>Key Laboratory of Multiscale Spin Physics, Ministry of Education,  
Beijing Normal University, Beijing 100875, China

We present the first alternative mechanisms to trigger black hole bomb phenomena beyond the famous superradiant instability. By incorporating nonlinear self-interaction into the massive charged scalar field in general relativity, we discover that the allowed static solutions suggest two such novel dynamic mechanisms, which are further confirmed by our numerical simulations. The first one originates from the linearly unstable hairy black hole, but the bomb can be avoided by dialing the coefficient of the tiny scalar pulse. This distinguishes it from superradiant instability, where the bomb is an inevitable destiny. The second one is an intrinsically nonlinear process, which can even drive a linearly stable Reissner-Nordström black hole to become a black hole bomb by releasing substantial energy to develop scalar hair. This is also in sharp contrast with superradiant instability which can only drive an unstable black hole. These findings not only open up new avenues for black hole energy burst, but also have potential implications for new phenomena occurring around astrophysical black holes.

*Introduction*—Energy extraction from black holes has always been a topic of great interest. Soon after Penrose’s proposal that scattering a massive object off a rotating black hole could extract energy [1, 2], it was shown that a similar process for energy extraction could also be implemented by scattering a charged object off a spherical charged black hole [3]. A wave analogue of the Penrose process is superradiance [4–7], where the amplified scattering wave carries energy away, causing the black hole to stabilize with slightly less energy [8–10].

An intriguing application of superradiance is to make a black hole bomb [6]. With the introduction of a reflecting boundary, the amplified wave can be reflected back towards the black hole. The amplification repeats, generating a superradiantly unstable black hole that continuously releases energy to the wave, resulting in a sharp growth of the wave. Reflection can be achieved by placing the black hole in an artificial reflecting cavity or in an anti-de Sitter spacetime [11]. A more natural approach involves the mass term in the wave equation for a massive bosonic field, which inherently provides an effective reflecting potential barrier [12].

With the backreaction of amplified waves on spacetime, the black hole bomb induced by superradiant instability will inevitably terminate at some point and

the unstable seed black hole must transition to a stable state. However, exploring the whole progression of this process is challenging due to the significant disparity in timescales between the field oscillations and the growth rates of instability [13–16]. Only a few numerical simulations have successfully simulated the full evolution of the superradiant instability in asymptotically flat spacetimes [17–20] or in anti-de Sitter spacetimes [21–23]. The simulations in asymptotically flat spacetimes show that energy can indeed be substantially extracted from the superradiantly unstable black holes, leading to the gradual transition to hairy black holes [16, 24] with smaller energy within the horizon.

For a long time, the creation of black hole bombs was understood only through the famous superradiant instability. In this *Letter*, we present two novel dynamical mechanisms that can also lead to black hole bomb phenomena, even within the simple framework of general relativity minimally coupled with a self-interacting massive charged scalar field. These mechanisms arise from the nonlinear self-interaction of the matter which is often neglected in studying the superradiant instability at the linear level [25]. We first disclose an intriguing linear instability in a branch of hairy black hole solutions. Depending on the coefficient of the tiny perturbation, this instability has two possible evolutionary directions. One leads to scalar hair collapse, while the other leads to scalar hair explosion and black hole energy burst. This makes it a novel mechanism for triggering a black hole bomb, distinct from the superradiant instability which can only result in hair explosion and energy burst. We further demonstrate that Reissner-Nordström (RN) black

\* zhangcy@email.jnu.edu.cn

† chenqian192@mails.ucas.ac.cn

‡ 223093@csu.edu.cn

§ ytian@ucas.ac.cn

¶ wang\_b@sjtu.edu.cn

\*\*\* hongbaozhang@bnu.edu.cn

holes are always linearly stable in this model, meaning the traditional creation of a black hole bomb from an RN black hole via superradiant instability is absent. Surprisingly, we can still create a bomb by injecting a strong scalar pulse into the RN black hole. The nonlinear effect of the scalar field can destroy the stability of the RN black hole and drive it into a hairy black hole by releasing substantial charge and energy to develop scalar hair. This process is intrinsically nonlinear and does not need an artificial reflecting cavity. In contrast, superradiant instability can only transform an unstable black hole into a hairy one and requires a reflecting cavity for spherical charged black holes [17, 18, 21]. To our knowledge, these two processes represent the first alternative mechanisms capable of inducing black hole bomb phenomena beyond the superradiant instability.

*Model*—The Lagrangian of the model we consider is (using units where  $c = G = 1$ )

$$\mathcal{L} = R - F_{\mu\nu}F^{\mu\nu} - D^\mu\psi(D_\mu\psi)^* - V(\psi), \quad (1)$$

where  $R$  is the Ricci scalar associated with the metric, the Maxwell field strength  $F_{\mu\nu} = \partial_\mu A_\nu - \partial_\nu A_\mu$  with  $A_\mu$  being the gauge potential, and the gauge covariant derivative  $D_\mu = \nabla_\mu - iqA_\mu$  with  $q$  the gauge coupling constant of the complex scalar field  $\psi$ . We focus on the potential  $V(\psi) = \mu^2|\psi|^2 - \lambda|\psi|^4 + \nu|\psi|^6$  with  $\mu$  the scalar field mass, and  $\lambda, \nu$  the positive parameters governing the self-interactions. This potential is widely used in studying Q-ball [26], a type of non-topological soliton which may naturally arise in the early universe and is a candidate for dark matter [27–30]. It has recently been found that the above nonlinear self-interaction enables this model to circumvent the no-hair theorem [31], allowing static hairy black hole solutions [32, 33].

To investigate the static and dynamical properties of the black holes, we use the spherical Painlevé-Gullstrand (PG) coordinates:

$$ds^2 = -(1 - \zeta^2)\alpha^2dt^2 + 2\alpha\zeta dtdr + dr^2 + r^2d\Omega^2, \quad (2)$$

where  $\alpha, \zeta$  are the metric functions dependent on  $t$  and  $r$ . This coordinate system is regular at the apparent horizon  $r_h$ , where  $\zeta(t, r_h) = 1$ . Taking the gauge potential  $A_\mu dx^\mu = Adt$  and introducing auxiliary variables  $\Pi = n^\mu D_\mu\psi$  and  $E = n^\mu F_{\mu r}$  with  $n^\mu = (\alpha^{-1}, -\zeta, 0, 0)$  the unit normal vector to the constant time slice, we get the following constraint equations

$$0 = \partial_r E + \frac{2E}{r} - \frac{q}{2}\text{Im}(\Pi\psi^*), \quad (3)$$

$$0 = \partial_r \zeta + \frac{\zeta}{2r} - \frac{r(\rho_\psi + E^2)}{2\zeta} - \frac{r\text{Re}(\Pi^*\partial_r\psi)}{2}, \quad (4)$$

$$0 = \partial_r \alpha + \frac{\alpha r\text{Re}(\Pi^*\partial_r\psi)}{2\zeta}, \quad (5)$$

$$0 = \partial_r A - \alpha E, \quad (6)$$

and evolution equations

$$0 = \partial_t\psi - iqA\psi - \alpha(\Pi + \zeta\partial_r\psi), \quad (7)$$

$$0 = \partial_t\Pi - \frac{\partial_r(\alpha(\Pi\zeta + \partial_r\psi)r^2)}{r^2} - iA\Pi q + \alpha\frac{\partial V}{\partial\psi^*}. \quad (8)$$

Here  $\rho_\psi = T_{\mu\nu}^\psi n^\mu n^\nu = (|\Pi|^2 + |\partial_r\psi|^2 + V)/2$  is the projection of the scalar field stress-energy tensor along  $n^\mu$ . Given the initial distribution of  $\psi$  and  $\Pi$ , we obtain  $E, \zeta, \alpha$  and  $A$  by solving the constraint equations (3,4,5,6) successively. The evolution equations (7,8) are then solved by Runge-Kutta method to get  $\Pi, \psi$  on the next time slice. By repeating this procedure, we can obtain the matter and metric data on all time slices.

At spatial infinity, Minkowski spacetime should be approached. This implies the following boundary conditions for solving the equations:

$$\zeta \rightarrow \sqrt{\frac{2M}{r}}, \quad A \rightarrow \Phi + \frac{Q}{r}, \quad E \rightarrow -\frac{Q}{r^2}, \quad \psi, \Pi \rightarrow 0, \quad (9)$$

where  $M$  and  $Q$  are the total mass and charge of the system, respectively.  $\Phi$  is the gauge potential and we take  $\Phi = 0$  hereafter. We also set  $\alpha = 1$  at infinity by fixing the auxiliary freedom of  $\alpha dt$  in PG coordinates.

We trace the dynamical evolution by the scalar field energy  $E_\psi = \frac{1}{4\pi} \int_{r_h}^\infty dV \rho_\psi$ , the black hole charge  $Q_h = \frac{1}{4\pi} \oint_{r_h} dS F_{\mu\nu} n^\mu s^\nu$  with  $s^\nu$  the outward pointing unit normal vector to the apparent horizon two-sphere [34], as well as the black hole mass, defined by the Christodoulou-Ruffini formula as  $M_B = M_h + \frac{Q_h^2}{4M_h}$  with  $M_h = \sqrt{S_h/16\pi}$  the irreducible mass and  $S_h = 4\pi r_h^2$  the apparent horizon area [8–10, 19, 20, 35]. There should be charge conservation  $Q_h + Q_\psi = Q$  during dynamical evolution, where  $Q_\psi = \frac{1}{4\pi} \int dV n^\mu j_\mu$  with  $j_\mu = -\frac{q}{2}\text{Im}(\psi^* D_\mu\psi)$  the charge current carried by the scalar field. This fact can be employed to monitor our numerical simulations.

*Bombs suggested by static solutions*—As alluded to before, due to the nonlinear self-interaction, the model we are considering allows not only the RN solution with  $\psi = 0$ , but also hairy black hole solutions. The hairy black hole solutions have a static geometry and stress-energy tensor while the scalar field oscillates as  $\psi(t, r) = \phi(r)e^{i\omega t + if(r)}$  in PG coordinates. Here  $f(r) \equiv q\chi(r) - \omega g(r)$  is a phase. It can be removed by a combination of the gauge transformation  $\psi \rightarrow \psi e^{-iq\chi}, A \rightarrow A - \partial_r\chi$  and the coordinate transformation  $t \rightarrow t + g(r)$ . The scalar field exhibits an asymptotic behavior  $\phi \rightarrow \frac{c_0 e^{-\mu_\infty r}}{r}$  at spatial infinity, where  $c_0$  is an irrelevant constant and  $\mu_\infty \equiv \sqrt{\mu^2 - \omega^2}$  is the effective mass of the complex scalar field. The bound  $\omega \leq \mu$  should be satisfied for static hairy solutions; otherwise the scalar field would have infinite total energy and thus unphysical. Regularity on the horizon requires that the frequency  $\omega$  satisfies the resonance condition  $\omega = qA(r_h)$ . Given the gauge coupling  $q$ , black hole horizon radius  $r_h$  and total charge  $Q$ , the static hairy solutions can be worked out by solving the static equations of motion with Newton-Raphson

method. Other quantities such as  $\omega$ ,  $Q_h$  and  $M_B$  can be derived from these solutions.

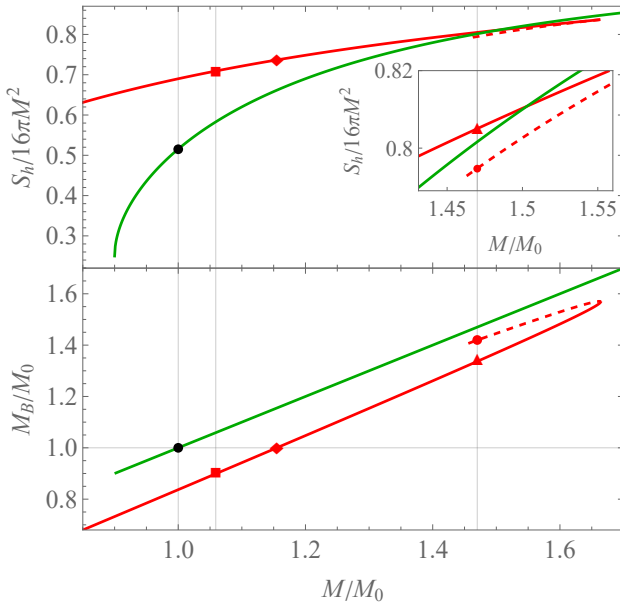


Figure 1. The black hole area  $S_h$  and mass  $M_B$  versus the total mass of the static black hole solutions with fixed  $Q = 0.9M_0$  when  $qM_0 = 3$ . The green line denotes the RN solutions, while the solid and dashed red lines represent the stable and unstable hairy black holes, respectively. The red and black points indicate the seed black holes in Figure 2 and 3, respectively.

Hereafter, we assume a reference RN black hole with a total mass  $M_0 = 1$  and a total charge  $Q_0 = 0.9M_0$ . The parameter  $M_0$  serves to establish the energy scale of the problem. Then we select the black hole solutions with a total charge  $Q$  identical to that of the reference black hole, but the total mass  $M$  can vary. The reason we fix  $Q = Q_0$  is to facilitate comparison with results from dynamical simulations later, where the total charge remains unchanged while the total mass  $M$  increases with perturbation strength. Without loss of generality, we further fix  $qM_0 = 3$  and the potential  $V(\psi) = \frac{|\psi|^2}{M_0^2}(1 - \frac{|\psi|^2}{0.1^2})^2$  which satisfies the weak and dominant energy conditions. Then the results for selected solutions with  $Q = Q_0$  are shown in Figure 1. Alongside the RN solution, two additional branches of hairy solutions emerge, coinciding at a certain maximum value of  $M$ . As displayed later, the dashed branch turns out to be linearly unstable, while the solid red branch and the RN branch are linearly stable. By organizing static solutions in such a fresh manner, we can readily argue for the feasibility of making black hole bombs through two potentially distinct mechanisms from the familiar superradiant instability.

Let us first start from the red point with  $M = 1.47M_0$ ,  $M_B = 1.42M_0$  on the dashed branch. Since this seed hairy black hole is linearly unstable, even a slight perturbation can drive it to one of two possible stable final states at  $M = 1.47M_0$ : either the stable hairy black

hole on solid red branch or the RN black hole on the green line. This speculation is supported by the fact that both of them have a larger horizon area  $S_h$  than the seed black hole. If the stable hairy black hole, as indicated by the red triangle, is the final state, then the unstable seed black hole must release substantial energy outward to transition to it, since the final state has a smaller black hole mass  $M_B$  within the horizon compared to the seed one. This implies a black hole bomb made from a linearly unstable hairy black hole.

On the other hand, it is also possible to make a black hole bomb out of an RN solution, say the black point with  $M = M_B = M_0$  on the green line. Although this seed RN black hole is linearly stable under a small perturbation, its stability under a large perturbation is not guaranteed. In particular, if we engineer the scalar field away from the realm of the validity of linear perturbation theory, with its charge density vanishing outside of the horizon, then according to the Penrose inequality ( $M \geq M_B$ ) [36–38], we can inject energy to make the total mass  $M$  of the system lie between  $M_0$  and  $1.155M_0$ , the value determined by the intersection diamond point of the horizontal gray line and the solid red curve. If this process can trigger the transition from the black point to a hairy black hole on the solid branch with  $M_0 < M < 1.155M_0$ , represented by the red square, then the linearly stable seed RN black hole with  $M_B = M_0$  must release a substantial amount of energy outward, since the final hairy black hole has  $M_B < M_0$  within the horizon. By this way, we can create a black hole bomb even from a linearly stable seed black hole. This intrinsically nonlinear process is permitted by the non-decreasing area law since the red square has a larger horizon area than the black point.

Below we shall confirm the above two novel dynamical mechanisms to make black hole bombs by our fully nonlinear numerical simulations, whereby we also find that both of them are controllable.

*Bombs confirmed by dynamical evolution*—We first confirm that the black hole bomb can be made out of the unstable hairy black hole. As such, we perturb the red point in Figure 1 with the following ingoing pulse

$$\delta\psi = pe^{-\frac{M_0}{r-r_1}-\frac{M_0}{r_2-r}} \frac{(r-r_1)(r_2-r)}{M_0^2}, \quad \delta\Pi = \partial_r \delta\psi, \quad (10)$$

if  $r_1 < r < r_2$  and zero otherwise. We fix  $r_1 = 4M_0$ ,  $r_2 = 9M_0$  in the simulations. With a tiny  $p$ , the increase in total mass is negligible. Typical simulations are shown in Figure 2. Depending on whether  $p$  is positive or negative, the unstable seed hairy black hole evolves into either an RN black hole or a linearly stable hairy black hole. When it evolves into the latter, the seed black hole releases a substantial amount of charge and energy into the scalar hair, similar to the black hole bomb triggered by superradiant instability. However, superradiant instability always results in scalar hair explosion and energy extraction from the black hole. Unlike this, here when the unstable seed hairy black hole instead evolves into an RN black hole, the scalar hair collapses rather than

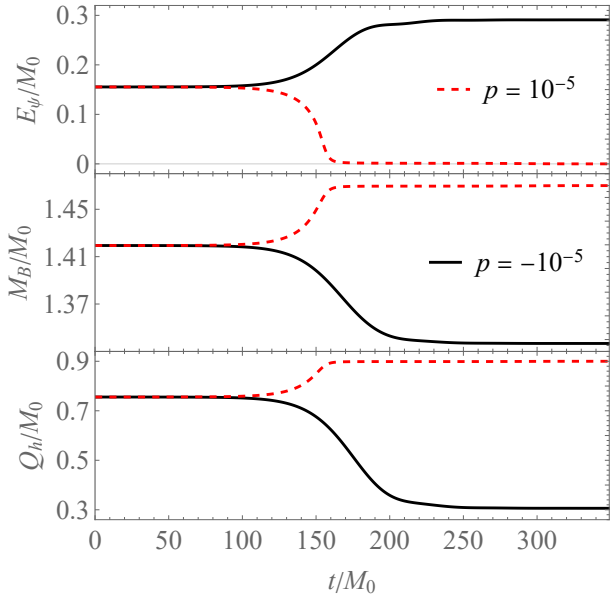


Figure 2. The evolution of scalar field energy  $E_\psi$ , black hole mass  $M_B$  and charge  $Q_h$  after the perturbation (10) with  $p = \pm 10^{-5}$  of the unstable hairy black hole with  $M = 1.47M_0$ ,  $M_B = 1.42M_0$  (red point in Figure 1). The corresponding total mass increment after perturbation is about  $10^{-7}M$ .

explodes, and its energy is absorbed by the black hole. This makes this linear instability a novel mechanism for triggering a black hole bomb beyond the superradiant instability. It is worth pointing out that this novel mechanism has the potential to extract up to 25% of the black hole energy, which occurs with a linearly unstable hairy extremal black hole with  $Q = M = 0.9M_0$  for smaller  $q$  such as  $qM_0 = 1$ .

To show that the bomb can also be made out of a linearly stable RN black hole, we inject the black point in Figure 1 with the following ingoing scalar pulse:

$$\delta\psi = 0.1pe^{-(\frac{r-12M_0}{2M_0})^2}, \quad \delta\text{II} = \partial_r\delta\psi. \quad (11)$$

The total mass increases with amplitude  $p$ , while the total charge is unchanged since the initial pulse has vanishing current  $\delta j_\mu$  everywhere. We plot the relevant result in Figure 3. For pulse (11), there exists a threshold  $p_1$ . When  $p < p_1$ , the scalar pulse is finally absorbed by the seed RN black hole, leading to another RN black hole with a larger black hole mass. This result is in accord with the fact that the RN black hole under consideration is linearly stable. Thus one cannot create a bomb from an RN black hole through the traditional superradiant instability in this model. However, for  $p > p_1$ , the strong nonlinear effect of the scalar field destroys the linear stability of the RN black hole and drives it to transition into a hairy black hole. In particular, when  $p_1 < p < 0.33$ , the final hairy black hole has a smaller mass  $M_B$  within the horizon than the seed black hole. Actually, up to 10% of the black hole energy and 80% of the black hole charge

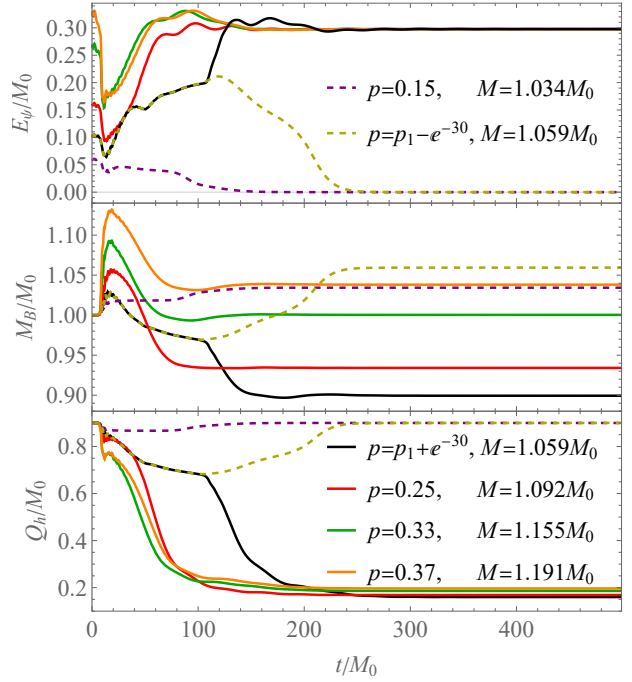


Figure 3. The evolution of scalar field energy  $E_\psi$ , black hole mass  $M_B$  and charge  $Q_h$  from an RN black hole with  $M = M_B = M_0$  (black point in Figure 1) under pulse injection (11). The dashed curves represent the evolution resulting in RN black holes, while the solid curves represent the evolution resulting in hairy black holes. The threshold  $p_1 \approx 0.198609115264384$  is determined with an accuracy up to order  $10^{-15}$  using the bisection method.

were extracted in our numerical simulations. This implies that we can create a black hole bomb in the nonlinear regime from an RN black hole, even it is linearly stable. But when  $p > 0.33$ , the total mass exceeds  $1.155M_0$ , so as illustrated in Figure 3 for  $p = 0.37$ , the final hairy black hole has a larger mass  $M_B$  than the seed black hole, which means no black hole bomb for larger  $p$ .

Therefore, we have fulfilled our promise made before. In particular, we find that the bomb made via either of the two novel mechanisms is controllable in the sense that it can be triggered only within the partial region of the parameter space of the scalar pulse profile.

*Conclusion*—Due to the nonlinear self-interaction of the massive charged scalar field, our model allows for not only RN solutions, but also two branches of hairy black hole solutions. This together with the non-decreasing area law as well as Penrose inequality suggests two novel dynamical mechanisms to create a black hole bomb, which is further confirmed explicitly by our fully nonlinear numerical simulations. The first one originates from the linearly unstable hairy black hole, but to be a bomb requires the coefficient of the scalar pulse profile be negative, which makes it distinct from the superradiant instability, whereby the bomb is unavoidable at all. The second one also differs from the superradiant instability, since it is triggered intrinsically in the nonlinear regime,

where the strong nonlinear self-interaction of scalar field can even drive a linearly stable RN black hole to transition into a hairy black hole by releasing substantial energy to develop scalar hair. As far as we know, these two processes are the first alternative mechanisms to the superradiant instability for creating a black hole bomb.

These findings highlight the significant impact of nonlinear self-interaction of matter fields on black hole energy burst. There are indications that analogous phenomena widely exist for black holes with other self-interacting massive solitary hairs, such as Proca and axion hair [39], which will be studied elsewhere in the future. On the other hand, given the mass gap between hairy and bald rotating black hole solutions [40–42], a tiny perturbation cannot transform a Kerr black hole to the hairy one. But the second mechanism which is intrin-

sically nonlinear as we disclosed here may apply to these black holes. In particular, with the involved matter field as a candidate for dark matter in mind, we have reason to expect that the vast energy burst induced by the novel mechanisms could produce intriguing observational signatures, which await to be further explored.

## ACKNOWLEDGMENTS

This work is supported by the Natural Science Foundation of China (NSFC) under Grant No. 12035016, 12075026, 12075202, 12375048, 12375058, and 12361141825, as well as the National Key R&D Program of China under Grant No. 2021YFC2203001.

---

[1] R. Penrose, *Gravitational collapse: The role of general relativity*, *Riv. Nuovo Cim.*, **1**, 252 (1969).

[2] R. Penrose and R. M. Floyd, *Extraction of rotational energy from a black hole*, *Nature*, **229**, 177 (1971).

[3] G. Denardo and R. Ruffini, *On the energetics of Reissner-Nordström geometries*, *Phys. Lett. B*, **45**, 259 (1973).

[4] Y. B. Zel'Dovich, *Generation of Waves by a Rotating Body*, Soviet Journal of Experimental and Theoretical Physics Letters, **14**, 180 (1971).

[5] C. W. Misner, *Interpretation of gravitational-wave observations*, *Phys. Rev. Lett.*, **28**, 994 (1972).

[6] W. H. Press and S. A. Teukolsky, *Floating Orbits, Superradiant Scattering and the Black-hole Bomb*, *Nature*, **238**, 211 (1972).

[7] J. D. Bekenstein, *Extraction of energy and charge from a black hole*, *Phys. Rev. D*, **7**, 949 (1973).

[8] W. E. East, F. M. Ramazanoğlu, and F. Pretorius, *Black Hole Superradiance in Dynamical Spacetime*, *Phys. Rev. D*, **89**, 061503 (2014), [arXiv:1312.4529 \[gr-qc\]](https://arxiv.org/abs/1312.4529).

[9] O. Baake and O. Rinne, *Superradiance of a charged scalar field coupled to the Einstein-Maxwell equations*, *Phys. Rev. D*, **94**, 124016 (2016), [arXiv:1610.08352 \[gr-qc\]](https://arxiv.org/abs/1610.08352).

[10] F. Corelli, T. Ikeda, and P. Pani, *Challenging cosmic censorship in Einstein-Maxwell-scalar theory with numerically simulated gedanken experiments*, *Phys. Rev. D*, **104**, 084069 (2021), [arXiv:2108.08328 \[gr-qc\]](https://arxiv.org/abs/2108.08328).

[11] S. W. Hawking and H. S. Reall, *Charged and rotating AdS black holes and their CFT duals*, *Phys. Rev. D*, **61**, 024014 (2000), [arXiv:hep-th/9908109](https://arxiv.org/abs/hep-th/9908109).

[12] T. Damour, N. Deruelle, and R. Ruffini, *On Quantum Resonances in Stationary Geometries*, *Lett. Nuovo Cim.*, **15**, 257 (1976).

[13] V. Cardoso and S. Yoshida, *Superradiant instabilities of rotating black branes and strings*, *JHEP*, **07**, 009 (2005), [arXiv:hep-th/0502206](https://arxiv.org/abs/hep-th/0502206).

[14] S. R. Dolan, *Instability of the massive Klein-Gordon field on the Kerr spacetime*, *Phys. Rev. D*, **76**, 084001 (2007), [arXiv:0705.2880 \[gr-qc\]](https://arxiv.org/abs/0705.2880).

[15] C. A. R. Herdeiro, J. C. Degollado, and H. F. Rúnarsson, *Rapid growth of superradiant instabilities for charged black holes in a cavity*, *Phys. Rev. D*, **88**, 063003 (2013), [arXiv:1305.5513 \[gr-qc\]](https://arxiv.org/abs/1305.5513).

[16] S. R. Dolan, S. Ponglertsakul, and E. Winstanley, *Stability of black holes in Einstein-charged scalar field theory in a cavity*, *Phys. Rev. D*, **92**, 124047 (2015), [arXiv:1507.02156 \[gr-qc\]](https://arxiv.org/abs/1507.02156).

[17] N. Sanchis-Gual, J. C. Degollado, P. J. Montero, J. A. Font, and C. Herdeiro, *Explosion and Final State of an Unstable Reissner-Nordström Black Hole*, *Phys. Rev. Lett.*, **116**, 141101 (2016), [arXiv:1512.05358 \[gr-qc\]](https://arxiv.org/abs/1512.05358).

[18] N. Sanchis-Gual, J. C. Degollado, C. Herdeiro, J. A. Font, and P. J. Montero, *Dynamical formation of a Reissner-Nordström black hole with scalar hair in a cavity*, *Phys. Rev. D*, **94**, 044061 (2016), [arXiv:1607.06304 \[gr-qc\]](https://arxiv.org/abs/1607.06304).

[19] W. E. East and F. Pretorius, *Superradiant Instability and Backreaction of Massive Vector Fields around Kerr Black Holes*, *Phys. Rev. Lett.*, **119**, 041101 (2017), [arXiv:1704.04791 \[gr-qc\]](https://arxiv.org/abs/1704.04791).

[20] W. E. East, *Massive Boson Superradiant Instability of Black Holes: Nonlinear Growth, Saturation, and Gravitational Radiation*, *Phys. Rev. Lett.*, **121**, 131104 (2018), [arXiv:1807.00043 \[gr-qc\]](https://arxiv.org/abs/1807.00043).

[21] P. Bosch, S. R. Green, and L. Lehner, *Nonlinear Evolution and Final Fate of Charged Anti-de Sitter Black Hole Superradiant Instability*, *Phys. Rev. Lett.*, **116**, 141102 (2016), [arXiv:1601.01384 \[gr-qc\]](https://arxiv.org/abs/1601.01384).

[22] P. M. Chesler and D. A. Lowe, *Nonlinear Evolution of the  $AdS_4$  Superradiant Instability*, *Phys. Rev. Lett.*, **122**, 181101 (2019), [arXiv:1801.09711 \[gr-qc\]](https://arxiv.org/abs/1801.09711).

[23] P. M. Chesler, *Hairy black resonators and the  $AdS_4$  superradiant instability*, *Phys. Rev. D*, **105**, 024026 (2022), [arXiv:2109.06901 \[gr-qc\]](https://arxiv.org/abs/2109.06901).

[24] C. Herdeiro, E. Radu, and H. Rúnarsson, *Kerr black holes with Proca hair*, *Class. Quant. Grav.*, **33**, 154001 (2016), [arXiv:1603.02687 \[gr-qc\]](https://arxiv.org/abs/1603.02687).

[25] R. Brito, V. Cardoso, and P. Pani, *Superradiance: New Frontiers in Black Hole Physics*, *Lect. Notes Phys.*, **906**, pp.1 (2015), [arXiv:1501.06570 \[gr-qc\]](https://arxiv.org/abs/1501.06570).

[26] S. R. Coleman,  *$Q$ -balls*, *Nucl. Phys. B*, **262**, 263 (1985), [*Addendum: Nucl.Phys.B* 269, 744 (1986)].

[27] J. A. Frieman, G. B. Gelmini, M. Gleiser, and E. W. Kolb, *Solitogenesis: Primordial Origin of Nontopological Solitons*, *Phys. Rev. Lett.*, **60**, 2101 (1988).

[28] T. D. Lee and Y. Pang, *Nontopological solitons*, *Phys. Rept.*, **221**, 251 (1992).

[29] A. Kusenko and P. J. Steinhardt, *Q ball candidates for selfinteracting dark matter*, *Phys. Rev. Lett.*, **87**, 141301 (2001), [arXiv:astro-ph/0106008](https://arxiv.org/abs/astro-ph/0106008).

[30] S. L. Liebling and C. Palenzuela, *Dynamical boson stars*, *Living Rev. Rel.*, **26**, 1 (2023), [arXiv:1202.5809 \[gr-qc\]](https://arxiv.org/abs/1202.5809).

[31] A. E. Mayo and J. D. Bekenstein, *No hair for spherical black holes: Charged and nonminimally coupled scalar field with selfinteraction*, *Phys. Rev. D*, **54**, 5059 (1996), [arXiv:gr-qc/9602057](https://arxiv.org/abs/gr-qc/9602057).

[32] C. A. R. Herdeiro and E. Radu, *Spherical electro-vacuum black holes with resonant, scalar Q-hair*, *Eur. Phys. J. C*, **80**, 390 (2020), [arXiv:2004.00336 \[gr-qc\]](https://arxiv.org/abs/2004.00336).

[33] J.-P. Hong, M. Suzuki, and M. Yamada, *Spherically Symmetric Scalar Hair for Charged Black Holes*, *Phys. Rev. Lett.*, **125**, 111104 (2020), [arXiv:2004.03148 \[gr-qc\]](https://arxiv.org/abs/2004.03148).

[34] J. M. Torres and M. Alcubierre, *Gravitational collapse of charged scalar fields*, *Gen. Rel. Grav.*, **46**, 1773 (2014), [arXiv:1407.7885 \[gr-qc\]](https://arxiv.org/abs/1407.7885).

[35] D. Christodoulou and R. Ruffini, *Reversible transformations of a charged black hole*, *Phys. Rev. D*, **4**, 3552 (1971).

[36] S. A. Hayward, *Inequalities relating area, energy, surface gravity and charge of black holes*, *Phys. Rev. Lett.*, **81**, 4557 (1998), [arXiv:gr-qc/9807003](https://arxiv.org/abs/gr-qc/9807003).

[37] M. M. Disconzi and M. A. Khuri, *On the Penrose Inequality for Charged Black Holes*, *Class. Quant. Grav.*, **29**, 245019 (2012), [arXiv:1207.5484 \[math.DG\]](https://arxiv.org/abs/1207.5484).

[38] S. McCormick, *On the charged Riemannian Penrose inequality with charged matter*, *Class. Quant. Grav.*, **37**, 015007 (2020), [arXiv:1907.07967 \[gr-qc\]](https://arxiv.org/abs/1907.07967).

[39] I. Salazar Landea and F. García, *Charged Proca Stars*, *Phys. Rev. D*, **94**, 104006 (2016), [arXiv:1608.00011 \[hep-th\]](https://arxiv.org/abs/1608.00011).

[40] C. Herdeiro, E. Radu, and H. Runarsson, *Non-linear Q-clouds around Kerr black holes*, *Phys. Lett. B*, **739**, 302 (2014), [arXiv:1409.2877 \[gr-qc\]](https://arxiv.org/abs/1409.2877).

[41] C. A. R. Herdeiro, E. Radu, and H. Rúnarsson, *Kerr black holes with self-interacting scalar hair: hairier but not heavier*, *Phys. Rev. D*, **92**, 084059 (2015), [arXiv:1509.02923 \[gr-qc\]](https://arxiv.org/abs/1509.02923).

[42] Y. Brihaye, C. Herdeiro, and E. Radu, *Myers-Perry black holes with scalar hair and a mass gap*, *Phys. Lett. B*, **739**, 1 (2014), [arXiv:1408.5581 \[gr-qc\]](https://arxiv.org/abs/1408.5581).

## SUPPLEMENTAL MATERIAL

We include supplemental material to demonstrate the results with varying parameters and scalar field potentials. This material unveils additional intriguing phenomena observed in the dynamical simulations and emphasizes the generality of our findings.

- *Simulations with a larger  $q$*

In the main text, we worked with  $V(\psi) = \frac{|\psi|^2}{M_0^2}(1 - \frac{|\psi|^2}{0.1^2})^2$  and  $qM_0 = 3$ . The results from these settings have led us to propose novel mechanisms for black hole bomb phenomena. Here we simulate the evolution with a larger

$q$  and showcase other intriguing dynamical phenomena that emerge during the evolution.

In Figure 4, we present the dynamical simulations using the same potential but with the parameter  $qM_0 = 5$ . In the upper panel, we observe that the scalar field energy  $E_\psi$ , black hole mass  $M_B$  and charge  $Q_h$  all experience rhythmic growths and declines over a long period. As depicted in the lower panel, this behavior is accompanied by the scalar field displaying prolonged rhythmic radial expansions and contractions during the evolution, reminiscent of the radial pulsations of Cepheid variable stars. To our knowledge, this is the first observation of such behavior in a black hole system. The radial expansions and contractions of the scalar field are due to the intense competition between the gravitational attraction and self-interaction versus the repulsion from energy extraction and electric forces. It suggests a time-dependent geometry that has not yet stabilized. In each cycle, a small amount of scalar field energy is absorbed by the central black hole. Eventually, a hairy black hole forms, characterized by a static geometry and stress-energy tensor while the scalar field continues to oscillate. Details of the final solutions are elaborated in the section "Bombs suggested by static solutions" in the main text.

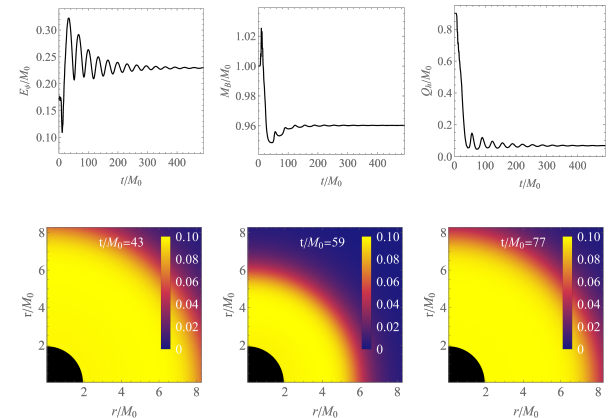


Figure 4. **Upper panel:** The evolution of the scalar field energy  $E_\psi$ , the black hole mass  $M_B$  and charge  $Q_h$  starting from an RN black hole with  $M_0 = 1, Q = 0.9M_0$  under the perturbation  $\delta\psi = 0.1pe^{-\frac{(r-12M_0)^2}{2M_0}}$ ,  $\delta\Pi = \partial_r\delta\psi$  with  $p = 0.26$  when  $qM_0 = 5$ . **Lower panel:** Snapshots of the absolute value  $|\psi|$  of the scalar field during the evolution. The black regions in the lower left corner represent the region inside the apparent horizon at the corresponding times.

- *Simulations with other potential*

We have focused on the potentials of the form  $V(\psi) = \mu^2|\psi|^2(1 - \frac{|\psi|^2}{\sigma^2})^2$ . However, the novel black hole bomb mechanisms we have discovered are not confined to this specific potential.

In Figure 5, we present results using a different potential  $V(\psi) = \frac{|\psi|^2}{M_0^2}(1 - \frac{2|\psi|^2}{0.1^2} + \frac{1.1|\psi|^4}{0.1^4})$  with  $qM_0 = 3$ . The left panel shows static black hole solutions with three branches, similar to those in Figure 1 of the main text,

indicating that the dynamical features are qualitatively similar across different scalar potentials. In the right panel, we indeed observe the same qualitative behavior as in Figure 3 of the main text: a sufficiently strong perturbation (with  $p = 0.3$ ) can trigger a black hole bomb from the linearly stable RN black hole, but an overly large perturbation (with  $p = 0.37$ ) results in no net energy extraction.

Additionally, selecting a seed black hole from the linearly unstable hairy black holes on the dashed branch leads to similar dynamical behaviors as shown in Figure 2 of the main text. For simplicity, we do not include these results here.

We have also tested the potential  $V(\psi) = \frac{|\psi|^2}{M_0^2}(1 - \frac{1.9|\psi|^2}{0.1^2} + \frac{|\psi|^4}{0.1^4})$  and obtained similar results. Note that all tested potentials satisfy the energy conditions. These experiments reinforce the generality of our findings across various potentials.

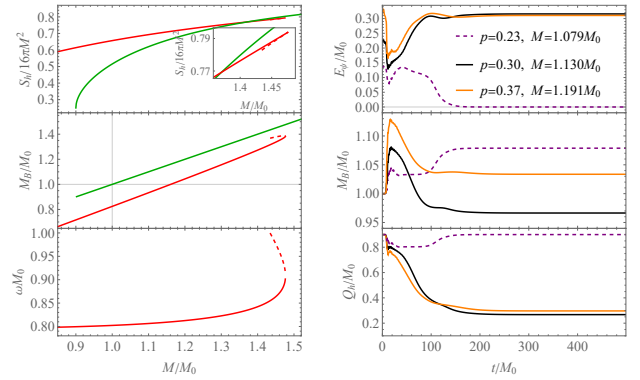


Figure 5. **Left panel:** Static black hole solutions with  $V(\psi) = \frac{|\psi|^2}{M_0^2}(1 - \frac{2|\psi|^2}{0.1^2} + \frac{1.1|\psi|^4}{0.1^4})$  and  $qM_0 = 3$ . The green line denotes the RN solutions, while the solid and dashed red lines represent the stable and unstable hairy black holes, respectively. The unstable hairy branch terminate at  $\omega M_0 = 1$  since the bound  $\omega \leq \mu = M_0^{-1}$  should be satisfied. All static solutions in the left panel have the same charge with a reference RN black hole which has a total mass  $M = M_0$  and a total charge  $Q = 0.9M_0$ . **Right panel:** The evolution of the scalar field energy  $E_\psi$ , the black hole mass  $M_B$  and charge  $Q_h$  starting from the reference RN black hole under the perturbation  $\delta\psi = 0.1pe^{-(\frac{r-12M_0}{2M_0})^2}$ ,  $\delta\Pi = \partial_r\delta\psi$  when  $qM_0 = 3$ .